

ARTICLES

Fast Energy Transfer of Charge–Transfer Triplet Excited State (^3CT) of $[\text{Ru}(\text{bpy})_3](\text{PF}_6)_2$ to Os^{2+} at Short Distances in the Crystal

Minoru Tsushima, Noriaki Ikeda,* Koichi Nozaki, and Takeshi Ohno*

*Department of Chemistry, Graduate School of Science, Osaka University, 1-16 Machikaneyama, Toyonaka, Osaka 560-0043, Japan**Received: October 11, 1999; In Final Form: February 1, 2000*

The energy transfer of a charge–transfer triplet excited state (^3CT) in $[\text{Ru}(\text{bpy})_3](\text{PF}_6)_2$ ($\text{bpy} = 2,2'$ -bipyridine) crystals doped with $[\text{Os}(\text{bpy})_3](\text{PF}_6)_2$ was studied by a time-correlated single-photon counting method, where the excited $\text{Ru}(\text{II})$ moiety and the $\text{Os}(\text{II})$ moiety act as energy donor (D) and acceptor (A), respectively. ^3CT of Ru^{2+} in the $[\text{Os}_x\text{Ru}_{1-x}(\text{bpy})_3](\text{PF}_6)_2$ ($x > 0.0099$) exhibited multiexponential decay, which is ascribed to direct energy transfer to Os^{2+} at various rates depending on the D – A distances. Hopping of ^3CT to the closest Ru^{2+} (Ikeda et al., *J. Phys. Chem. A*, 2000) changed the D – A distances and made the decay faster at a later time. The complex emission decay was analyzed by a Monte Carlo simulation. The rates of energy transfer to Os^{2+} at 0.82 and 1.08 nm were determined to be 1.7×10^{11} and $7 \times 10^9 \text{ s}^{-1}$, respectively. The distance dependence of the rates of energy transfer through space and its mechanism are discussed.

I. Introduction

Fast detection methods of reaction intermediates, such as time-resolved absorption spectroscopy and time-correlated single-photon counting, have provided unimolecular rates of electron transfer or energy transfer reactions occurring in donor–acceptor linked compounds. It has been shown for solution reactions of donor–acceptor metal complexes linked by a bridging group that the rate of either energy or electron transfer is strongly dependent on the bridging ligands.^{1–9} As for radiationless (back-electron transfer) transition of excited donor–acceptor complexes in solution, the disappearance of donor–acceptor interaction and the promoting of the plane–plane stretching vibration mode are responsible for the fast electron transfers.^{10–12}

It could be of crucial importance to investigate the relation between the rate of bimolecular reaction and the degree of intermolecular electronic coupling in crystals that are doped with acceptor or are composed of a donor and an acceptor. Both the distance and the orientation between a donor and an acceptor could be related to rates of intermolecular reactions. However, few studies on intermolecular reactions in crystalline solid have been done because (1) reactions between molecules in close proximity are too fast to be detected, (2) time-resolved absorption spectroscopy has been rarely applied to solid-state reactions because of thermal decomposition of the sample following the photoexcitation,¹³ and (3) the rate of photoinduced intermolecular reaction could not be extracted by analysis of multiexponential decays of emission for crystalline solids.¹³

Spectroscopic studies of the charge–transfer triplet excited state (^3CT) of $[\text{Ru}(\text{bpy})_3]^{2+}$ in the crystalline state have been performed at very low temperature to identify the lowest excited state and to elucidate the emission mechanism from the excited state.^{14–17} There are some arguments whether the ^3CT state of

$\text{Ru}(\text{II})$ as a luminophore in the concentrated or neat crystal is localized or its excitation energy can migrate.^{18–20} More recently, it has been demonstrated that the ^3CT of $[\text{Ru}(\text{bpy})_3](\text{PF}_6)_2$ migrates to undergo an energy transfer reaction to an acceptor and annihilation reaction with another ^3CT , and the rate constants of excitation hopping to the metal ion sites of crystal are dependent on the site–site distances of crystal.¹³

Here, an energy transfer process in the $[\text{Ru}(\text{bpy})_3](\text{PF}_6)_2$ crystal doped with $[\text{Os}(\text{bpy})_3](\text{PF}_6)_2$ (Os^{2+}) of various mole fractions has been studied. The multiexponential decay of emission ascribable to the various rates of energy transfer to Os^{2+} sites at different distances has been accurately measured by a cavity-dumped Ti^{3+} :sapphire laser and time-correlated single-photon counting technique. The rates of energy transfers to Os^{2+} at the various distances were determined by a Monte Carlo (MC) simulation for the multiexponential decay of emission.

II. Experimental Section

A. Materials. The compounds, $[\text{M}(\text{bpy})_3](\text{PF}_6)_2$ ($\text{M} = \text{Ru}, \text{Os}$) were prepared by metathesis from $[\text{Ru}(\text{bpy})_3]\text{Cl}_2 \cdot 6\text{H}_2\text{O}$ ²¹ and $[\text{Os}(\text{bpy})_3]\text{I}_2 \cdot 3\text{H}_2\text{O}$ ²² salts that were synthesized according to literature methods and then recrystallized from acetonitrile–ethanol solution. The crystals of $[\text{Ru}(\text{bpy})_3](\text{PF}_6)_2$ doped with $[\text{Os}(\text{bpy})_3](\text{PF}_6)_2$ were prepared from acetonitrile–ethanol solution after mixing the solution of each component in the stoichiometric molar ratio. The doping concentration of the highly doped crystal was determined by measuring the absorption spectra of the solution in which the doped crystal was redissolved. Because the crystal structure of $[\text{Os}(\text{bpy})_3](\text{PF}_6)_2$ as a guest molecule is isomorphous with that of $[\text{Ru}(\text{bpy})_3](\text{PF}_6)_2$ as a host crystal and those cell parameters are almost the

same,^{23,24} it is assumed that doping and mixing between these two compounds to form crystals is homogeneous.

B. Apparatus and Measurements. Absorption spectra were recorded on Shimadzu MPS-2000 or UV2500PC spectrophotometers. Emission spectra of the crystals were measured with a grating polychromator (Jasco CT250) with a silicon diode array (Hamamatsu S3901–512Q). The 488 nm line of an Ar laser was used for the excitation. Crystal samples were normally contained in 2-mm diameter quartz cells under atmospheric conditions. For measuring the emission spectra of a single crystal at room temperature, only the front surface of the crystal, which was placed on a fine glass tip with an angle of 45° against the excitation light, was excited with an objective lens ($\times 10$), and the emission from the same surface of the crystal was detected. The detector sensitivity was corrected with a Bromine lamp (Ushio JPD 100V500WCS). For measuring the emission decays under weak excitation power¹³ with high time resolution, the following time-correlated single-photon counting system with a cavity-dumped Ti^{3+} :sapphire laser was used.

C. Cavity-Dumped Ti^{3+} :Sapphire Laser. A Kerr lens mode-locked Ti^{3+} :sapphire laser with a cavity dumper was home-built according to literatures methods.^{25–27} The laser was pumped with all lines (6 W) from an argon ion laser (Coherent Innova 306). The Ti^{3+} :sapphire laser ($4\phi \times 20$ mm rod; SF10 prism spacing, 35 cm) routinely produces pulses of 80–100 fs duration with 76 MHz.^{25,26} The addition of the cavity dumper, which consists of a fused-silica Bragg Cell (Harris H101) and a radio frequency wave driver (CAMAC CD5000) with booster amplifier (CAMAC PB1800), allows deflection of the intracavity energy out of the oscillator, yielding 10–20 nJ/pulse at 800 nm with variable repetition rates (1.9 MHz–9.5 kHz).²⁷ For the usual measurements, the repetition rate was set at 200 kHz with 40–50% dumping efficiency. The laser output pulse (800 nm) was frequency doubled to 400 nm by a BBO crystal (Type I, 7 mm thick).

D. Time-Correlated Single-Photon Counting System. The fundamental and second harmonics of the laser were separated by a beam splitter. The fundamental was monitored with a high-speed photodiode (PD, Hamamatsu C4258) for starting pulse, and the 400-nm light was used for the sample excitation. The emission from samples was detected with a monochromator (Jobin Yvon HR10) with a microchannel plate photomultiplier (MCP–PM, Hamamatsu R3809U-51X) that is cooled. Signals from the PD (start pulse) and the MCP–PM (stop pulse) were amplified with preamplifiers (EG&G Ortec VT120B and 9306, respectively) and then discriminated with ps-timing discriminators (EG&G Ortec 9307). Those output pulses were fed into a time-to-amplitude converter (TAC, EG&G Ortec 567). The output of the TAC was directed to a high-rate multichannel buffer (EG&G Ortec spectrum master 921) and then transferred to a computer for data storage, display, and analysis. The full width at half-maximum (fwhm) of instrumental response function (IRF) in our system is typically 40 ps. The IRF varies sometimes in the experiments, and it was always characterized prior to each experiment. The emission decay were convoluted with the IRF.

III. Results and Discussion

A. Multiexponential Decay of Emission. The emission of the single crystal of $[\text{Os}_x\text{Ru}_{1-x}(\text{bpy})_3](\text{PF}_6)_2$ ($x = 0.0099–0.231$) consists of two peaks at 17 500 and 14 500 cm^{-1} that are assigned to the phosphorescence¹⁷ from the $^3\text{CT}(\text{Ru})$ and $^3\text{CT}(\text{Os})$ states, respectively. The occurrence of energy transfer from

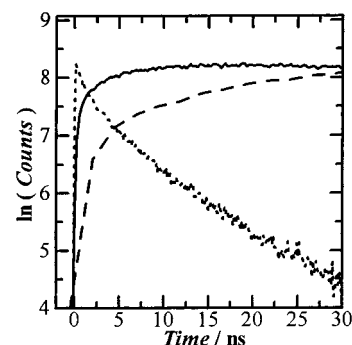


Figure 1. Decay of the emission of $[\text{Ru}(\text{bpy})_3]^{2+}$ at 600 nm for the single crystal of $[\text{Os}_{0.048}\text{Ru}_{0.952}(\text{bpy})](\text{PF}_6)_2$ is shown in the dotted line. The emission rises of $[\text{Os}(\text{bpy})_3]^{2+}$ for the single crystals of $[\text{Os}_{0.048}\text{Ru}_{0.952}(\text{bpy})_3](\text{PF}_6)_2$ and $[\text{Os}_{0.0099}\text{Ru}_{0.99}(\text{bpy})_3](\text{PF}_6)_2$ are shown in the solid line and in the broken line, respectively. The temperature was 298 K.

a $^3\text{CT}(\text{Ru})$ to an $\text{Os}(\text{II})$ in the doped crystal was detected by observing the enhancement of the $\text{Os}(\text{II})$ emission along with a decrease of the $\text{Ru}(\text{II})$ emission when the doping concentration of $\text{Os}(\text{II})$ was increased. A rise of the $\text{Os}(\text{II})$ emission accompanied by decay of the $\text{Ru}(\text{II})$ emission within 5×10^{-9} s after the laser excitation confirmed the energy transfer, as is shown in Figure 1. The presence of Os^{2+} in the crystal of $[\text{Os}_x\text{Ru}_{1-x}(\text{bpy})_3](\text{PF}_6)_2$ shortened the duration of emission at 600 nm as the doping concentration increased. The emission decay curves of $[\text{Ru}(\text{bpy})_3](\text{PF}_6)_2$ are multiexponential in a wide range of the doping concentration of Os^{2+} .

$$I(t) = \sum_{n=1} A_n \exp(-k_n t) \quad (1)$$

where A_n and k_n stand for the initial amplitude and the rate constant of the n^{th} decay component, respectively.

As far as the slowest decay component is concerned, the decay rates were dependent on the doping concentration of Os^{2+} . A good linearity of the rate constant of the slowest decay component to the concentration of Os^{2+} suggests that ^3CT undergoes hopping sequentially to the closest metal ion sites of crystal to eventually encounter an Os^{2+} in a process analogous to free diffusion in a solution of an excited-state donor.¹³ The rate constant of the hopping in the crystal of $[\text{Ru}(\text{bpy})_3](\text{PF}_6)_2$ was estimated to be $3.6 \times 10^8 \text{ s}^{-1}$ from the rate constants of the second-order reactions, energy transfer to Os^{2+} , and annihilation of $^3\text{CT}(\text{Ru})$ in $[\text{Ru}(\text{bpy})_3](\text{PF}_6)_2$.¹³ However, the total decay curves of $\text{Ru}(\text{II})$ emission were never described in biexponential function, and the decay rates in an early time region (< 1 ns) could not be determined for the crystal of $[\text{Os}_x\text{Ru}_{1-x}(\text{bpy})_3](\text{PF}_6)_2$ ($x > 0.0099$). Only the times for the emission intensity of the fast decay component ($I(0)$) to decrease to $I(0)/e$ were evaluated, yielding 44, 5.1, 0.73, and 0.29 ns for the crystals containing the mole fractions of Os^{2+} of 0.0099, 0.048, 0.115, and 0.231, respectively.

B. Monte Carlo Simulation of Emission Decay. All the $^3\text{CT}(\text{Ru})$ undergo intrinsic decay, energy transfer to an Os^{2+} in the metal ion sites at various distances (r), and hopping to Ru^{2+} in the nearest metal ion sites. The number of metal ion sites at a distance (z) is given from the crystallographic data of $[\text{Ru}(\text{bpy})_3](\text{PF}_6)_2$,²³ as shown in Table 1. The emission decay resulting from the first two processes ($I(t)$) is statistically written

TABLE 1: Ten Kinds of the Smallest Separation Distances (r) and the Number of Metal Ion Sites (z) in the $[\text{Ru}(\text{bpy})_3](\text{PF}_6)_2$ Crystal Calculated from the Crystallographic Data^a

parameter	value									
r , nm	0.820	1.076	1.352	1.640	1.864	1.961	2.036	2.152	2.303	2.460
z	2	6	12	2	6	12	12	6	12	2

^a Reference 23.

in terms of occupation probability (x) of Os(II) in the metal ion sites of $[\text{Os}_x\text{Ru}_{1-x}(\text{bpy})_3](\text{PF}_6)_2$

$$I(t) = I(0)\exp(-k_0t)[1 - x + x \exp(-k_{\text{en}}(0.82)t)]^2 \times [1 - x + x \exp(-k_{\text{en}}(1.076)t)]^6 \times [1 - x + x \exp(-k_{\text{en}}(1.352)t)]^{12} \times [1 - x + x \exp(-k_{\text{en}}(r)t)]^2 \dots \quad (2)$$

where $k_{\text{en}}(r)$ are the rate constants of energy transfer depending on the distance (r) between $^3\text{CT}(\text{Ru})$ and an Os(II). The first exponential term of the right-hand side represents the intrinsic decay in neat crystal. The first and the second square brackets of the right-hand side represent the reaction of energy transfer to Os^{2+} at the nearest metal ion sites and the second nearest metal ion sites, respectively. Consequently, the decay of emission is multiexponential, and the rate of the emission decay decreases with time. In an early stage of time, ^3CT surrounded by Os^{2+} at short distances undergoes energy transfer to decay. ^3CT surrounded by Os^{2+} at long distances are left to decay slowly in a later stage of time. If ^3CT surrounded by Os^{2+} at long distances migrates by a hopping to encounter an Os^{2+} , the rate of energy transfer in a later stage of time is enhanced. This enhancement is the case, because the rate of the hopping to the nearest Ru^{2+} was estimated to be much larger ($3.6 \times 10^8 \text{ s}^{-1}$) than the intrinsic decay rate. The simple statistical equation (eq 2) is not valid any more.

To reconstitute the decay profile of emission, the time for deactivation of a ^3CT was calculated by considering only the rate constants for intrinsic decay, energy transfer, and hopping, the latter two of which depend on the distances $^3\text{CT}-\text{Os}^{2+}$ and $^3\text{CT}-\text{Ru}^{2+}$, respectively. Monte Carlo simulation of the emission decay was performed by assuming the stochastic processes of intrinsic decay, energy transfer to an Os^{2+} , and excitation hopping to the closest Ru^{2+} sites of crystal. The $\text{Ru}(\text{II})$ are randomly excited to $^3\text{CT}(\text{Ru})$ in a volume of 1.25×10^5 lattices based on the crystallographic data, where a periodic boundary condition is introduced and the Os^{2+} are also randomly distributed in the same volume. The occurrence of deactivation of every ^3CT in a short time interval (δt) was stochastically determined based on the presumed rate constants of energy transfer ($k_{\text{en}}(r)$) to Os^{2+} at distance (r) and the intrinsic decay of ^3CT as follows. If a random number generated between 0 and 1 is smaller than the probability of deactivation, $1 - \exp[-(k_0 + k_{\text{en}}(r))\delta t]$, the excited donor can be regarded as being deactivated in a time interval of δt (3 ps). The time interval was 3 ps in which only 3% of ^3CT underwent energy transfer to Os^{2+} of the largest mole fraction (0.231). The energy transfer to Os^{2+} until at the 10th nearest metal ion sites were considered. Once the excited donor was in a similar way determined to undergo the excitation hopping to the nearest metal ion sites in the time interval based on the rate constant of k_{hop} ($3.6 \times 10^8 \text{ s}^{-1}$), the recalculated distances between the $^3\text{CT}(\text{Ru})$ and Os^{2+} vary the rates of energy transfer to Os^{2+} in the succeeding time. The lifetimes of the excited donors were determined in the stochastic way. The summing up of the lifetimes over all the ^3CT (1.25×10^3) gives rise to the decay profile of emission as shown in Figures 2 and 3.

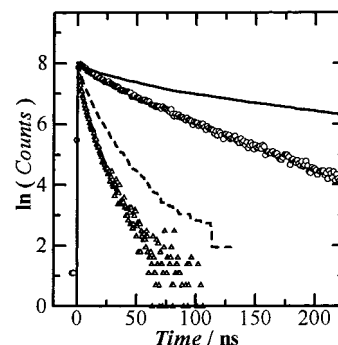


Figure 2. Emission decay curves of the highly doped $[\text{Os}_x\text{Ru}_{1-x}(\text{bpy})_3](\text{PF}_6)_2$ at 298 K. Both the observed decay curves (triangles: $x = 0.048$ and circles: $x = 0.0099$) and the stochastically simulated curves (dashed line: $x = 0.048$ and solid line: $x = 0.0099$) are shown for the comparison. The magnitudes of energy-transfer to Os^{2+} at 0.82 and 1.08 nm, evaluated by eq 3, are 9.8×10^8 and $1.8 \times 10^8 \text{ s}^{-1}$, respectively. The rate constants of hopping to Ru^{2+} at 0.82 and 1.08 nm are 3.6×10^8 and $1.8 \times 10^7 \text{ s}^{-1}$, respectively. The simulated curves were convoluted by the IRF.

C. Monte Carlo Simulation of Emission Decay via Förster Mechanism of Energy Transfer. Distance-dependent rate constants of energy transfer are calculated based on Förster mechanism of donor–acceptor interaction. The rate of resonance energy transfer, $k_{\text{en}}(r)$, from the $^3\text{CT}(\text{Ru})$ to Os(II) is estimated by using the following equation²⁸

$$k_{\text{en}}(r) = \frac{9000\phi_{\text{D}} \ln 10\kappa^2}{128\pi^5 N\tau_{\text{D}}n^4 r^6} \int \frac{f_{\text{D}}(\bar{\nu})\epsilon_{\text{A}}(\bar{\nu})}{\bar{\nu}^4} d\bar{\nu} \quad (3)$$

where τ_{D} , ϕ_{D} , $f_{\text{D}}(\bar{\nu})$, and $\epsilon_{\text{A}}(\bar{\nu})$ are the lifetime of donor emission, the quantum yield of donor emission, the spectral distribution of the donor emission normalized to unity, and the molar extinction coefficient for the absorption band of the acceptor at wavenumber ($\bar{\nu}$), respectively. The orientation factor (κ^2) is 2/3 based on the assumption of random distribution. The refractive index of the crystal medium (n) is set to 1.5. The overlap integral between the $\text{Ru}(\text{II})$ emission and the Os(II) absorption is calculated to be $4 \times 10^{-14} \text{ mol}^{-1}\text{cm}^{-6}$.¹³ The emission yield of $[\text{Ru}(\text{bpy})_3](\text{PF}_6)_2$ in crystal is assumed to be 0.163 by using the relation, $\phi_{\text{D}} = \tau_{\text{D}}/\tau_0$, where τ_0 is the natural lifetime (15 μs).^{29,30} By using the optimum values, the optimum rate of energy transfer at 0.82 and 1.076 nm (k_{en}) are 9.8×10^8 and $1.8 \times 10^8 \text{ s}^{-1}$, respectively.

The calculated decay profiles of emission in an early stage deviates from that observed, as shown in Figure 2. The slower rate constants of energy transfer to Os^{2+} in close proximity are responsible for the discrepancy.

D. Monte Carlo Simulation of Emission Decay via Dexter and Förster Mechanisms of Energy Transfer. An alternate interaction scheme involved an electron exchange interaction between reactants at short distances (Dexter mechanism).³¹ The rate constant due to this interaction is given as follows

$$k_{\text{en}}(r) = k_{\text{en}}^0 \exp[-\beta_{\text{en}}(r - 0.6)] \quad (4)$$

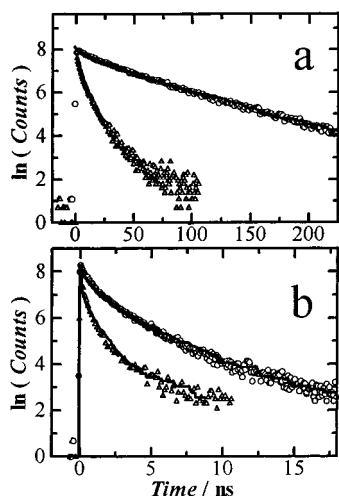


Figure 3. Emission decay curves of the highly doped [Os_xRu_{1-x}(bpy)₃](PF₆)₂ at 300 K: (a) the observed ones (circles and triangles) are for $x = 0.0099$ and $x = 0.048$, respectively, and the Monte Carlo simulated ones (solid line); (b) the observed one (circles and triangles) are for $x = 0.115$ and $x = 0.231$, respectively, and the Monte Carlo simulated ones (solid line). The magnitudes of $k_{\text{en}}(r)$ are evaluated with eq 4, for the pairs of Ru(II)–Os(II) closer than 1.64 nm and by with eq 3 for the other pairs of Ru(II)–Os(II). The magnitude of k_{hop} (1.08) are evaluated with eq 5. The best fitted parameters are as follows: $k_{\text{en}}^0 = 2.7 \times 10^{12} \text{ s}^{-1}$, $\beta_{\text{en}} = 12.5 \text{ nm}^{-1}$, and $\beta_{\text{hop}} = 11.5 \text{ nm}^{-1}$. The simulated curves were convoluted by the IRF.

where β_{en} and k_{en}^0 are, respectively, an attenuation factor and the rate constant of energy transfer to Os²⁺ at the contact distance of 0.6 nm. The contact distance for the energy transfer is set to the van der Waals radius of the complex cation. To simulate the much faster decay of emission in the early time region, the rate constants of Dexter-type energy transfer to Os²⁺ at the short distances of 0.82, 1.08, and 1.35 nm were considered. The rate constants of energy transfer to Os²⁺ at distances > 1.35 nm were presumed to be dominated by the Förster mechanism. The hopping to the second closest site at 1.08 nm is also considered for the simulation because the hopping to the second closest neighbor sites could not be considered insignificant for the crystals doped with low fractions of Os²⁺ (0.046 and 0.0099). The rate constants for hopping are given by using a similar attenuation factor to that for energy transfer to Os²⁺, as in eq 4

$$k_{\text{hop}}(r) = 3.6 \times 10^8 \exp[-\beta_{\text{hop}}(r - 0.82)] \quad (5)$$

The same parameter set of k_{en}^0 ($2.7 \times 10^{12} \text{ s}^{-1}$), β_{en} (12.5 nm^{-1}), and β_{hop} (11.5 nm^{-1}) gives the best fitting for the emission decays of the crystals doped with Os²⁺ of different mole fractions ($x = 0.231, 0.115, 0.048$, and 0.0099), as is shown in Figure 3. Because 88% of ³CT(Ru) in the crystal doped with Os²⁺ of the largest mole fraction (0.231) is transferred to Os²⁺ at the closest and the second closest sites,³² the simulation is dependent on the magnitudes of both k_{en} (0.82) and k_{en} (1.08). Similarly, because 70% and 53% of ³CT(Ru) in the crystal

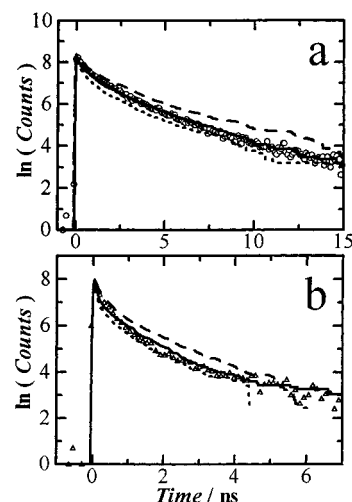


Figure 4. Sensitivity of the Monte Carlo simulation of emission decay to β_{en} and k_{en}^0 . (a) The open circles are the observed one for [Os_{0.115}Ru_{0.885}(bpy)₃](PF₆)₂ and the lines are calculated with k_{en}^0 ($2.7 \times 10^{12} \text{ s}^{-1}$), β_{hop} (11.5 nm^{-1}), and β_{en} (10.5 nm^{-1} for the dotted one, 12.5 nm^{-1} for the solid one, and 13.0 nm^{-1} for the dashed one). (b) The triangles are the observed ones for [Os_{0.231}Ru_{0.769}(bpy)₃](PF₆)₂. The lines are calculated with β_{en} (12.5 nm^{-1}), β_{hop} (11.5 nm^{-1}), and k_{en}^0 ($1 \times 10^{12} \text{ s}^{-1}$ for the dotted line, $2.7 \times 10^{12} \text{ s}^{-1}$ for the solid line, and $4 \times 10^{12} \text{ s}^{-1}$ for the dashed line).

doped with Os²⁺ of mole fractions, 0.115 and 0.048, respectively, are transferred to Os²⁺ at the second and the third closest sites,³² the processes involving k_{en} (1.08), k_{en} (1.35), and k_{hop} (1.08) were included in the simulations. As is shown in Figure 4, the sensitivity of the calculated curves is very high to the extents of β_{en} and β_{hop} (not shown) for the decays in the crystal doped with Os²⁺ of mole fractions (0.115 and 0.048), whereas the dependence of the calculated curve on the extent of k_{en}^0 is weak even for the decay in the crystal highly doped with Os²⁺.

E. Distance-Dependent Rates of Energy Transfer to Os²⁺ and Hopping to Ru²⁺. By using the parameters obtained in the stochastic simulation, the distance-dependent energy transfer rates via the exchange–interaction mechanism³¹ are estimated as $k_{\text{en}}(0.82) = 1.7 \times 10^{11} \text{ s}^{-1}$, $k_{\text{en}}(1.08) = 7 \times 10^9 \text{ s}^{-1}$, and $k_{\text{en}}(1.35) = 2.2 \times 10^8 \text{ s}^{-1}$, which are much larger than the rates (1.2×10^9 , 2.4×10^8 , and $6.2 \times 10^7 \text{ s}^{-1}$, respectively) calculated assuming dipole–dipole interaction (see Table 2). As for the hopping to the second closest sites, the rate constant is estimated to be $1.8 \times 10^7 \text{ s}^{-1}$. The exchange–interaction with an acceptor at distances > 1.35 nm is relatively inefficient. Nevertheless, the energy transfer to an Os²⁺ at 1.64 and at 1.86 nm via the Förster mechanism (1.9×10^7 and $9.0 \times 10^6 \text{ s}^{-1}$, respectively) does not always take place because the excitation hopping to the metal sites at the closest distance ($3.6 \times 10^8 \text{ s}^{-1}$) is much faster than the energy transfers.

The value derived for the distance attenuation factor (12.5 nm^{-1}) is somewhat smaller than that (20 nm^{-1}) for energy transfer in chemically linked donor(Ru²⁺)–acceptor(Fe²⁺) compounds in solution.³⁴ The present authors are investigating

TABLE 2: Best Fit Parameters, (k_{en}^0 , β_{en} , and β_{hop}), Used in the Monte Carlo Simulation (left) and the Rate-Constants of Energy Transfer and Hopping Calculated from the Parameters for the Closest Pairs (right)

parameters			rate constants of energy transfer and hopping				
k_{en}^0 , 10^9 s^{-1}	β_{en} , nm^{-1}	β_{hop} , nm^{-1}	k_{en} (0.82), 10^9 s^{-1}	k_{en} (1.08), 10^9 s^{-1}	k_{en} (1.35), 10^9 s^{-1}	k_{hop} (0.82), 10^9 s^{-1}	k_{hop} (1.08), 10^9 s^{-1}
2700	12.5	11.5	170	7.0	0.22	0.36 ^a	0.018

^a Reference 13.

the rate of similar energy transfer in other crystalline solid to clarify the distance dependence of the energy transfer rate.

Because the rate of energy transfer can be generally written as the product of exchange interaction and Franck–Condon factor between a donor and an acceptor, the large rate of the energy transfer can be ascribed to a large spectral overlap integral and/or a large exchange integral. Although the energy acceptors of the processes for energy transfer and excitation hopping are different (Os^{2+} and Ru^{2+} , respectively), the inner d-orbitals of the metal ions but the outer p-orbitals of bpy ligands could interact with those of ${}^3\text{CT}$ commonly between the processes. Therefore, the difference in the extent of exchange interaction between two pairs, $\text{Ru(II)}-\text{Os(II)}$ and $\text{Ru(II)}-\text{Ru(II)}$, cannot account for the big difference in the rate between the energy transfer ($1.7 \times 10^{11} \text{ s}^{-1}$) and the hopping ($3.6 \times 10^8 \text{ s}^{-1}$). The larger contributing factor might be a difference in Franck–Condon factor between the processes, although the evaluation of Franck–Condon factor for the hopping of ${}^3\text{CT}(\text{Ru})$ is too small to be evaluated.

IV. Conclusions

Observed multiexponential decays of emission in crystals of $[\text{Ru}(\text{bpy})_3](\text{PF}_6)_2$ doped with Os(II) of various mole fractions ($x = 0.0099, 0.046, 0.115, \text{ and } 0.23$) were examined by means of a Monte Carlo simulation. The rates of the fast energy transfer to Os^{2+} at 0.82 and at 1.08 nm were determined to be 1.7×10^{11} and $7 \times 10^9 \text{ s}^{-1}$, respectively, from the distance attenuation factor and the maximum rate of energy transfer to Os^{2+} at the van der Waals distance. A distance attenuation factor (12.5 nm^{-1}) for the electronic exchange interaction in the purely through-space system is small compared with reference values. It is shown that the electron-exchange interaction is predominant for the fast energy transfer of ${}^3\text{CT}(\text{Ru})$ to Os^{2+} and for the hopping of ${}^3\text{CT}(\text{Ru})$ to the closest metal ion sites in the crystal.

Acknowledgment. We thank Dr. S. Adachi and Prof. Y. Takagi of Himeji Institute of Technology, and Mr. T. Ariyoshi, Prof. S. Kinoshita, and Dr. Y. Nagasawa of Osaka University for giving the technical comments of laser construction. The present work was partially supported by Grants-in-Aid from the Japanese Ministry of Education, Science, Sports, and Culture to N.I.

References and Notes

- (1) (a) Balzani, V.; Scandola, F. *Supramolecular Photochemistry*; Horwood: Chichester, UK, 1992. (b) Sauvage, J.-P.; Collin, J.-P.; Chambron, J.-C.; Guillerez, S.; Coudret, C.; Balzani, V.; Barigelli, F.; De Cola, L.; Flamigni, L. *Chem. Rev.* **1994**, *94*, 993. (c) Voegtle, F.; Frank, M.; Nieger, M.; Belser, P.; von Zelewsky, A.; Balzani, V.; Barigelli, B.; De Cola, L.; Flamigni, L. *Angew. Chem. Int. Ed. Engl.* **1993**, *32*, 1643.
- (2) Furee, M.; Yoshidzumi, T.; Kinoshita, S.; Kushida, T.; Nozakura, S.; Kamachi, M. *Bull. Chem. Soc. Jpn.* **1991**, *64*, 1632.
- (3) (a) Nozaki, K.; Ohno, T.; Haga, M. *J. Phys. Chem.* **1992**, *96*, 10880. (b) Yoshimura, A.; Nozaki, K.; Ikeda, N.; Ohno, T. *J. Phys. Chem.* **1996**,

- 100*, 1630. (c) Nozaki, K.; Ikeda, N.; Ohno, T. *New J. Chem.* **1996**, *20*, 739.
- (4) (a) Yoshimura, A.; Nozaki, K.; Ikeda, N.; Ohno, T. *Bull. Chem. Soc. Jpn.* **1996**, *69*, 2791. (b) Gholamkhash, B.; Nozaki, K.; Ohno, T. *J. Phys. Chem.* **1997**, *101*, 9010.
- (5) De Cola, L.; Balzani, V.; Barigelli, F.; Flamigni, L.; Belser, P.; von Zelewsky, A.; Frank, A.; Voegtle, A. *Inorg. Chem.* **1993**, *32*, 5228.
- (6) Larson, S. L.; Hendrickson, S. M.; Ferrere, S.; Derr, D. L.; Elliott, C. M. *J. Am. Chem. Soc.* **1995**, *117*, 5881.
- (7) Beley, M.; Chodorowski, M.; Collin, J.-P.; Sauvage, J. P.; Flamigni, L.; Barigelli, F. *Inorg. Chem.* **1994**, *33*, 2543.
- (8) Grosshenny, V.; Harriman, A.; Hissler, M.; Ziessel, R. *J. Chem. Soc., Faraday Trans.* **1996**, *92*, 2223.
- (9) Schantz, K. S.; Cabana, L. A. *J. Phys. Chem.* **1990**, *94*, 2740.
- (10) Hubig, S. M.; Kochi, J. K. *J. Phys. Chem.* **1995**, *99*, 17578.
- (11) Rubtsov, I. V.; Yoshihara, K. *J. Chem. Phys. A* **1997**, *101*, 6138.
- (12) Asahi, T.; Matsuo, Y.; Masuhara, H.; Kojima, H., *J. Phys. Chem. A* **1997**, *101*, 612.
- (13) Ikeda, N.; Tsushima, M.; Yoshimura, A.; Ohno, T. *J. Phys. Chem. A*, in press.
- (14) Yersin, H.; Braun, D. *Coord. Chem. Rev.* **1991**, *111*, 39.
- (15) Krausz, E.; Ferguson, J. *Prog. Inorg. Chem.* **1989**, *37*, 293.
- (16) Krausz, E.; Riesen, H. *Coord. Chem. Rev.* **1997**, *159*, 9.
- (17) Krol, D. M.; Blasse, G. *Chem. Phys. Lett.* **1981**, *77*, 253.
- (18) (a) Yersin, H.; Braun, D.; Gallhuber, E.; Hensler, G.; Ber. Bunsenges. Phys. Chem. **1987**, *91*, 1228. (b) Yersin, H.; Hensler, G.; Gallhuber, E. *Inorg. Chim. Acta* **1987**, *132*, 187.
- (19) Yersin, H.; Hensler, G.; Gallhuber, E.; Rettig, W.; Schwan, L. O. *Inorg. Chim. Acta* **1987**, *105*, 201.
- (20) Krausz, E.; Nightingale, T. *Inorg. Chim. Acta* **1986**, *120*, 37.
- (21) Palmer, R. A.; Piper, T. S. *Inorg. Chem.* **1966**, *5*, 864.
- (22) Burstall, F. J.; Dwyer, F. P.; Gyarfus, E. C. *J. Chem. Soc.* **1950**, 953.
- (23) (a) Rillema, D. P.; Jones, D. S. *J. Chem. Soc., Chem. Comm.* **1979**, 849. (b) Biner, M.; Burgi, H.-B.; Ludi, A.; Rohr, C. *J. Am. Chem. Soc.* **1992**, *114*, 5197.
- (24) (a) Constable, E. C.; Raithby, P. R.; Smit, D. N. *Polyhedron* **1989**, *8*, 367. (b) Richter, M. M.; Scott, B.; Brewer, K. J.; Willett, R. D. *Acta Crystallogr.* **1991**, *C47*, 2443.25.
- (25) (a) Spence, D. E.; Kean, P. N.; Sibbet, W. *Opt. Lett.* **1991**, *16*, 42. (b) Murnane, M. M.; Kapteyn, H. C.; Huang, C. P.; Asaki, M. T. Mode-Locked Ti:Sapphire Laser, Washington State University, Internal Report, Rev.1.7 1994.
- (26) (a) Takagi Y.; Adachi, S., private communication. (b) Ariyoshi, T.; Kinoshita, S. *J. Spectrosc. Soc. Jpn.* **1997**, *46*, 196.
- (27) (a) Pshenichnikov, M. S.; de Boeij, W. P.; Wiersma, D. A. *Opt. Lett.* **1994**, *19*, 572. (b) Jonas, D. M.; Lang, M. J.; Nagasawa, Y.; Joo, T.; Fleming, G. R. *J. Phys. Chem.* **1996**, *100*, 12660.
- (28) Forster, Th. H. *Discuss. Faraday Soc.* **1959**, *27*, 7.
- (29) Islam, A.; Ikeda, N.; Nozaki, K.; Ohno, T. *Chem. Phys. Lett.* **1996**, *263*, 209.
- (30) (a) Harrigan R. H.; Crosby, G. A. *J. Chem. Phys.* **1973**, *59*, 3468. (b) Hager, G. D.; Crosby, G. A. *J. Am. Chem. Soc.* **1975**, *97*, 7031.
- (31) Dexter, D. C. *J. Chem. Phys.* **1953**, *21*, 836.
- (32) Because the rate of energy transfer to Os^{2+} at the shortest sites is much faster than that at the next shortest ones, the energy transfer occurs to an Os^{2+} at the shortest site if at least one of these sites is occupied by an Os^{2+} . The probabilities of an Os^{2+} occupying the shortest and the second shortest sites in the crystal doped with Os^{2+} of 0.231 are calculated to be $0.41 = 1 - (1 - 0.231)^2$ and $0.47 = (1 - 0.231)^2(1 - (1 - 0.231)^6)$, respectively.³³
- (33) Sykora, M.; Kincaid, J. R.; Dutta, P. K.; Castagnola, N. B. *J. Phys. Chem. B* **1999**, *103*, 309.
- (34) The value of β_{en} should be estimated by multiplying the original value⁶ by $\log_e 10$.